

Linear Friction Welding of a 2024 Al Alloy: Microstructural, Tensile and Fatigue Properties

Fabio Rotundo¹, Alessandro Morri², Lorella Ceschini²

¹DIEM, University of Bologna V.le Risorgimento 2, Bologna, I-40136, Italy

²SMETEC, University of Bologna V.le Risorgimento 4, Bologna, I-40136, Italy

Keywords: Metal Matrix Composites (MMCs), Friction welding, Mechanical properties

Abstract

The possibility of using linear friction welding (LFW) to produce high quality joints on an aerospace grade aluminium alloy (AA2024) was evaluated. In this solid state joining process the bonding of two flat edged components is achieved through frictional heating, induced by their relative reciprocating motion, under an axial compressive force. The Al joints were subjected to microstructural and mechanical characterization, including hardness and tensile tests. S–N probability curves were also computed after preliminary axial fatigue tests. No post-weld heat treatment was performed. The microstructural analyses showed substantially defect-free joints, with a relevant plastic flow in the thermo-mechanically altered zone. Maximum hardness decrease in the joint zone was approximately only 5% in respect to the base material. The joint efficiency was about 90% with respect to the ultimate tensile strength, with a slight reduction in the elongation to failure. Good fatigue performances were also detected.

Introduction

The difficulties in welding aerospace grade aluminium alloys, such as 2XXX (Al-Cu) and 7XXX (Al-Zn-Mg) series, have hitherto limited their use in structural applications [1]. In particular, the use of traditional fusion welding techniques generally leads to microstructural defects such as: high porosity, oxide inclusions and solidification shrinkage, as well as distortions. As a consequence, the resulting joints is characterized by a significant decrease of the mechanical properties with respect to the base material [2].

These fusion-related microstructural defects can be significantly reduced by the use of solid state joining techniques, such as friction welding, characterized by a high repeatability and excellent properties of the joints. Further advantages are due to the fact that no special preparation of the components is needed, no shielding gas is required and no, or little, pollution and waste are produced. Among different friction welding techniques, friction stir welding (FSW) has been successfully applied to a

wide range of Al alloys [1]. Although limited in the case of unreinforced Al alloys, one of the drawbacks of FSW is the wear of the pin, which could lead to Fe entrapment in the welded zone and due to pin shape variation, void formation in the weld nugget [3]. Moreover, slight asymmetries arise from the different relative speed of the pin on the two welding sides.

These problems could be solved by means of another friction welding technique, which do not need any consumable tool, the Linear Friction Welding, which extends the application of Rotary Friction Welding techniques to non-axisymmetric components.

In the LFW process, one component is oscillated linearly and brought in contact with the other component, which is rigidly clamped and pushed against the moving piece. Frictional heating is supplied as a consequence of the concurrent action of the increasing axial force (resulting in increasing pressure at the interface) and linear reciprocating motion. The true contact area increases and, as soon as sufficient material plasticization is achieved, the deformed material is expelled as flash, leading to an axial shortening which increases linearly with time [4]. As the imposed axial shortening (burn-off distance) is achieved, the reciprocating motion is stopped, and a forging force is applied to obtain sound joints, inducing further axial shortening.

Although the effects of FSW on different Al alloys have already been discussed [1], LFW has been generally applied only to Ti alloys [5], steels [6], Ni-based superalloys [7] and, by the authors, to a 2124Al/SiC_p composite [4, 8].

The aim of this work is to evaluate the effects of linear friction welding on the microstructure and mechanical behavior, including tensile and fatigue properties, of a 2024 Al alloy.

Experimental

The 2024 Al alloy, whose nominal chemical composition is reported in Table 1, was supplied as extruded rectangular plates, T4 heat treated.

LFW joints, with 15x36 mm² cross-section, were realized with Linear Friction Welding at TWI (The Welding Institute, Cambridge, UK), according to the scheme shown in Fig.1.

	Cr	Cu	Fe	Mg	Mn	Si	Ti	Zn	Other	Al
AA2024	≤0.10	3.80-4.90	≤0.50	1.20-1.80	0.30-0.90	≤0.50	≤0.15	≤0.25	≤0.15	Bal.

Table 1. Nominal chemical composition (wt.%) of the AA2024.

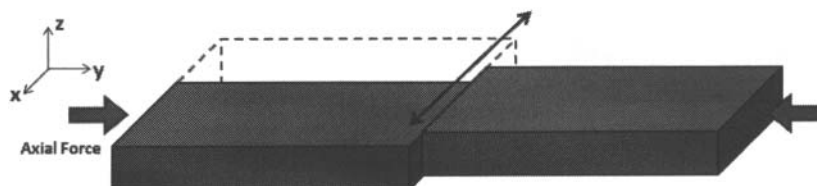


Fig. 1. Linear friction welding schematic.

After some preliminary tests, welding parameters were set-up, as following: oscillation frequency of 50 Hz, amplitude of ± 2 mm, axial force of 85 kN. Neither mechanical nor chemical treatments of the metal surfaces were applied before welding and no post-weld heat treatment was carried out.

Samples for microstructural investigations were cut along the y-z plane of Fig.1. The metallographic samples were mechanically ground, coarse polished and chemically etched with Keller's reagent. The microstructural characterization was carried out by optical microscopy (OM) under polarized light and scanning electron microscopy (SEM) with an energy dispersive spectroscopy (EDS) microprobe.

Vickers hardness measurements were taken across the joints, with a 5 kg load (HV_5), on a central line parallel to the y axis, in the transverse cross-sections used for the microstructural analyses.

Flat dog-bone specimens, with a gauge length of 12 mm, were machined according to ISO/TTA2 [9] for tensile and fatigue tests, with the main axis perpendicular to the welded x-z plane, shown in Fig. 1. A total of 9 specimens underwent tensile tests, at a strain rate of 10^{-4} s^{-1} , on a servo-hydraulic machine equipped with a 100 kN load cell and a clip-on extensometer.

For fatigue tests, in order to remove the effects of the CNC machining process, specimens were polished with abrasive papers of decreasing roughness, until reaching a final surface roughness lower than $R_a = 0.2 \mu\text{m}$. Fatigue tests were carried out under stress control, on a servo-hydraulic testing machine, equipped with a 100 kN load cell. Sinusoidal waveform, at a cyclic frequency of 20 Hz and a load ratio $R = 0$, were used. The run-out was set at 10^7 cycles. A total of 25 specimens underwent axial fatigue tests, with the maximum load distributed between 140 MPa and 300 MPa, and a load step of 20 MPa. The *maximum likelihood method* was used to analyze the fatigue data and to determine the S-N probability curve [4]. This method allows for the consideration of fatigue tests in which specimens survive achieving run-out which, on the contrary, cannot be considered to compute S-N curves when using a least square method.

SEM analyses of the fracture surfaces, following tensile and fatigue tests, were carried out to understand the underlying failure mechanisms.

Results and discussion

Linear friction joints were characterized by the presence of flash material extruded both parallel and normally with respect to the force-motion plane (x-y), as shown in Fig. 2.

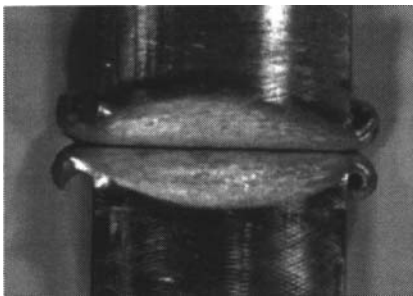


Fig. 2. AA2024 LFW joints shape.

Microstructural analyses

Microstructural characterization showed the relevant plastic deformation which the LFW process induced in the joints. Three

characteristic zones were identified in the joint (Fig. 3): *weld centre*, whose width varies along the weld line, where relevant grain refinement is likely to occur, as a consequence of the concurrent action of frictional heating and severe plastic deformation; *thermo-mechanically affected zone* (TMAZ), where the grain orientation follows the high temperature plastic flow; *heat affected zone* (HAZ), where no plastic deformation occurs, but thermal cycling affects the material properties.

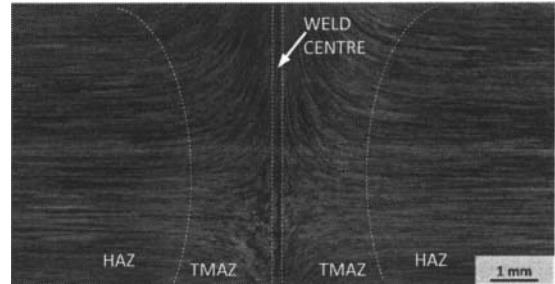
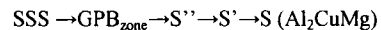


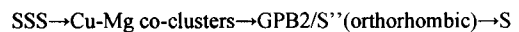
Fig. 3. Optical micrograph of the joint cross section.

Hardness

HV_5 profile is reported in Fig. 4. With respect to the base material, the joint hardness is slightly higher in the weld centre, while a decrease of approximately 5% was measured in the TMAZ. The hardness profile is related to the complex microstructural modifications induced by LFW, with the concurrent effects of frictional heating and severe plastic deformation, that lead to grain refinement and possible modification of the intermetallic strengthening phases. The age hardening mechanisms of Al-Cu-Mg alloys, such as AA2024, is still under discussion in the literature, both in the initial and peak stages. Main precipitation sequence, according to the classic approach of Bagaryatsky [9], is the following:



where SSS represents supersaturated solid solution and GPB Guinier-Preston-Bagaryatsky zones. Wang et al. [11, 12] recently suggested a slightly different precipitation sequence, considering that there is no evidence for the existence of GPB zones, and the S' precipitate has the same structure as the S phase, with only a slight difference in their lattice parameters. According to this approach, Cu-Mg co-clusters originate during initial natural aging, which, during artificial aging, are dissolved and replaced by S (Al_2CuMg) precipitates, which in turn coarsen after longer time exposure at high temperature:



Similarly to what as reported by Genevois et al. for the FSW case [13], it is possible to hypothesize that the LFW induces Cu-Mg co-clusters dissolution in the HAZ and, if the temperature is high enough, precipitation and coarsening of the S phase, with a consequent hardness decrease. In the TMAZ, the higher temperature leads to the formation of coarser S precipitates, with further hardness reduction. Although for a short time, the higher temperature achieved in the weld centre, during the LFW process, could, on the contrary, dissolve both the Cu-Mg co-clusters and the S precipitates.

As a consequence, the subsequent post-weld natural aging can lead to the formation of new Cu-Mg co-clusters [4], which determine, with the concurrent effect of grain refinement induced

by dynamic recrystallization and presence of Cu-Mg co-clusters, the higher hardness in the weld centre, in respect to the TMAZ.

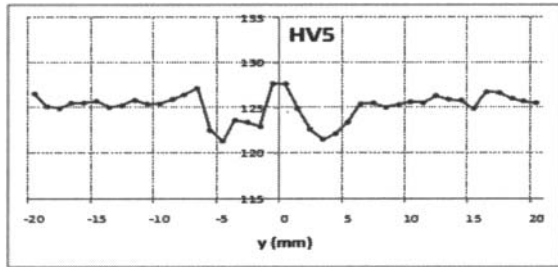


Fig. 4. HV₅ hardness profile on the cross-section of the AA2024 LFW joints.

Tensile properties

Tensile test results of the LFW joints showed excellent efficiencies calculated with respect to the base material, supplied at the same conditions, considering in particular that no post-weld heat treatment was performed. In particular, the ultimate tensile strength was found to be 428 MPa, with a 92% efficiency, while the R_{p02} yield strength resulted 309 MPa, with a 95% joint efficiency. Elongation to failure higher than 10% was also found, despite the fibrosity perpendicular to the tensile load application, induced by the welding process.

Fatigue properties

The experimental fatigue data and corresponding statistical analysis, with S-N curve at 50 % failure probability, are reported in Fig. 5. Fatigue strength at 10⁷ cycles corresponded to 152 MPa. This high fatigue resistance is related to the absence of welding defects and fine joint microstructure, as later confirmed by the analysis of the fracture surfaces.

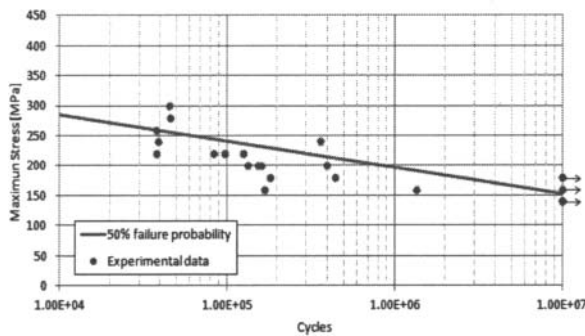


Fig. 5. Axial fatigue tests and S-N curve.

Fracture surface analyses

In the tensile specimens of the AA2024 LFW joints, fracture usually occurred between the TMAZ and central zone (Fig. 6-a), where the grains are oriented perpendicularly to the applied load. Only in a few specimens, fracture occurred between the TMAZ and HAZ (Fig. 6-b). The different possible location of the fracture path could be related to the previously discussed hardness profile fluctuations.

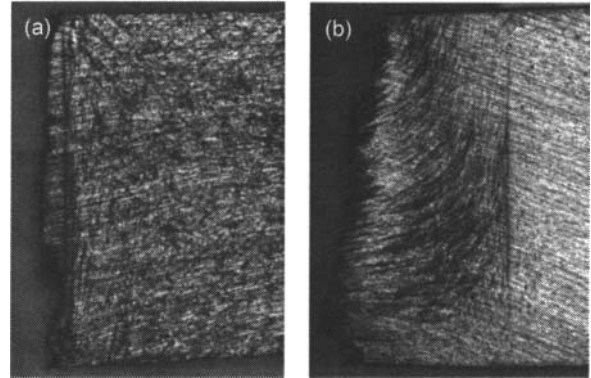


Fig. 6. Tensile fracture locations.

When fracture path crossed the weld centre, SEM analyses of the fracture surfaces showed an area that is macroscopically flat. When observed at greater magnification, this area was found to be characterized by fine dimples, with size smaller than 1 μm, supporting the hypothesis that a substantial grain refinement occurred in the weld centre during the LFW process (Fig. 7).

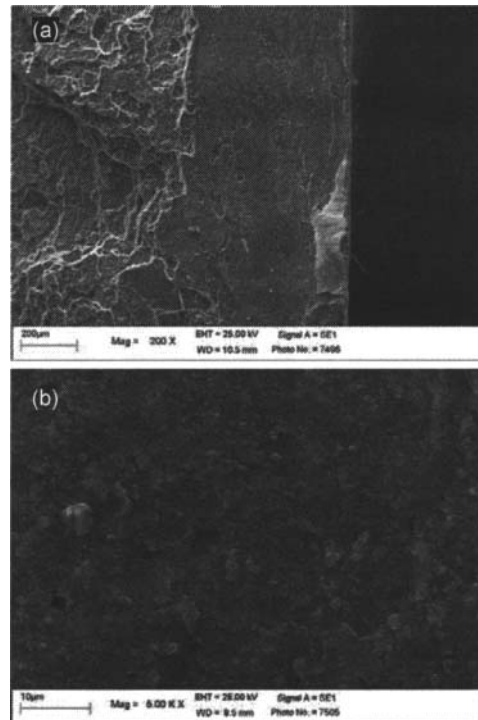


Fig. 7. Representative SEM micrographs of the fracture surfaces of the LFW AA2024 tensile specimens.

As for tensile specimens, also in the fatigue tests fracture usually occurred between the TMAZ and central zone. Fig. 8 shows how crack propagates on several cleavage planes at different heights, with an intergranular fracture mode.

Fracture nucleation is often triggered in correspondence of Cu-based precipitate clusters. Very rarely, oxide inclusions were found at crack nucleation site.

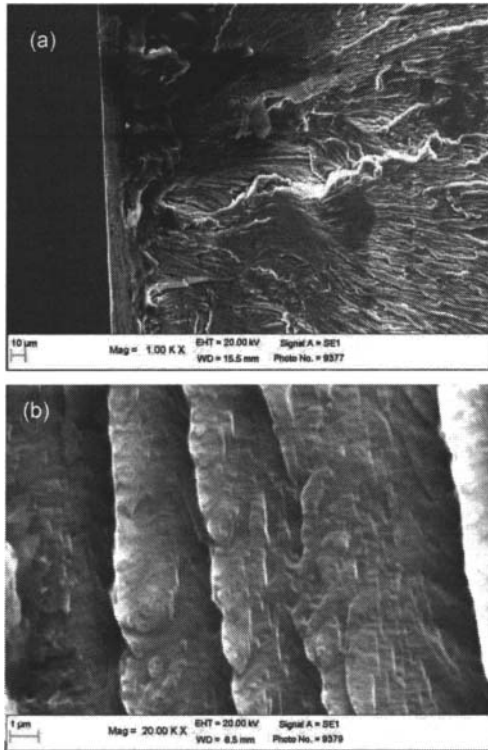


Fig. 8. Representative SEM micrographs of the fracture surfaces of the LFW AA2024 fatigue specimens.

Conclusions

The experimental results shown in this paper demonstrated Linear Friction Welding to be an attractive technology to join aerospace grade Al alloys. In particular, sound joints were produced from a T4 heat-treated AA2024, and no post-weld heat treatment was performed.

Microstructural analyses showed substantially defect-free joints. Three characteristic zones were identified in all the LFW specimens: weld centre, with an ultra-fine microstructure; thermo-mechanically affected zone (TMAZ) with severe plastic deformation; heat-affected zone (HAZ), without visible microstructural modifications. The hardness decrease was limited to approximately 5% in respect to the base material. The efficiency of the LFW joints was higher than 90%, in respect to the tensile and fatigue strength. Good fatigue performance were shown, with a fatigue resistance of 152 MPa at a 10^7 cycles (50% failure probabilities). The analyses of the fracture surfaces evidenced the presence of several cleavage planes, with fracture usually located between the TMAZ and the weld centre.

References

1. R.S. Mishra, Z.Y. Ma, *Friction stir welding and processing*, Material Science and Engineering, 50 (1-2) (2005), 1–78.
2. R.P. Matrukanitz, *Selection and weldability of heat-treatable aluminum alloys*, ASM Handbook—Welding, Brazing and Soldering 6 (1990) 528–536.
3. W.M. Zeng, H.L. Wu, J. Zhang, *Effect of tool wear on microstructure, mechanical properties and acoustic emission of*

- friction stir welded 6061 Al alloy*, Acta Metallurgica Sinica (English Letters) 19 (1) (2006), 9–19.
4. F. Rotundo, L. Ceschini, A. Morri, T-S. Jun, A.M. Korsunsky, *Mechanical and microstructural characterization of 2124Al/25 vol.%SiCp joints obtained by linear friction welding (LFW)*, Composites: Part A, 41 (2010), 1028–1037.
5. A. Vairis, M. Frost, *High frequency linear friction welding of a titanium alloy*. Wear, 217 (1998), 117–31.
6. W.Y. Li, T.J. Ma, S.Q. Yang, Q.Z. Xu, Y. Zhang, J.L. Li, *Effect of friction time on flash shape and axial shortening of linear friction welded 45 steel*, Material Letters, 62 (2) (2008), 293–6.
7. M. Karadge, M. Preuss, P.J. Withers, S. Bray, *Importance of crystal orientation in linear friction joining of single crystal to polycrystalline nickel-based superalloys*. Material Science and Engineering A, 491 (1-2) (2008), 446–53.
8. Jun TS, Rotundo F, Song X, Ceschini L, Korsunsky AM. *Residual strains in AA2024/AlSiCp composite linear friction welds*, Materials and Design, 31 (1) (2010), S117-S120.
9. ISO/TTA 2. *Tensile tests for discontinuously reinforced metal matrix composites at ambient temperatures*. (1997)
10. Y. A. Bagaryatshy, Dokl Akad. *Structural changes on Aging Al-Cu-Mg alloys*, SSSR, (87) 1952, 397-559.
11. S.C. Wang, M-J. Starink, *The assessment of GPB2/3 structures in Al-Cu-Mg alloys*, International Materials Reviews, 50 (2005), 193-215.
12. S.C. Wang, M-J. Starink, N. Gao, *Precipitation hardening in Al-Cu-Mg alloys revisited*, Scripta Materialia, 54 (2006), 287–291.
13. C. Genevois, D. Fabrègue, A. Deschamps, W.J. Poole, *On the coupling between precipitation and plastic deformation in relation with friction stir welding of AA2024 T3 aluminum alloy*, Materials Science and Engineering A, 441 (2006), 39–48.